Dynamic Simulator for Advanced Gas Turbine Engine Component Tests

R. A. Cundiff* and R. H. Badgley†
Mechanical Technology, Inc., Latham, N.Y.
and
J. Reddecliff‡
United Aircraft Corporation, West Palm Beach, Fla.

A rotor-bearing system has been designed and manufactured to be dynamically representative of an entire class of gas turbine engines: the two-spool front-drive, power-turbine engine, which is widely used in helicopter applications. The test rig configuration, with the addition of low-pressure compressor and fan simulator disks, would be dynamically representative of the turbojet and turbofan classes of engines, respectively. The simulator has been designed to permit developmental testing and evaluation of a number of advanced components and procedures. Among these are advanced intershaft bearings, rolling-element bearing dampers, and advanced balancing procedures. The apparatus has been utilized to date for initial evaluation of air-lubricated intershaft foil bearings, and for demonstration of an advanced balancing procedure. For these tests, the shaft was operated on elastically-mounted ball bearings without support damping over a speed range encompassing two bending critical speeds. Rotor balancing via the recently-developed multiplane-multispeed balancing procedure was used to suppress both the first bending critical speed and a pedestal resonance, and to leave a distinct vibration peak at the second bending critical speed. An air-lubricated intershaft foil bearing of the hydrodynamic, resiliently-supported type proved to be capable of raising the second critical speed above the normal operating speed range of the power turbine shaft.

Introduction

Gas Turbine Engine Rotor Dynamics

WITH the advent of higher performance, more compact two-spool gas-turbine engines which employ higher rotational speeds and higher temperatures, adequate control of the dynamics of the inner rotor is becoming more and more difficult to achieve. This is because inner shafts supported on two bearings tend to have one or more flexible critical speeds within the engine operating speed range.

This problem has been traditionally solved by either increasing the shaft diameter, adding bearings and bearing support structure, or by utilizing an appropriate number of rolling-element intershaft bearings. By proper placement of these bearings, the flexibility of the inner shaft is controlled and vibration amplitudes are maintained within acceptable limits.

Alternate approaches to inner spool rotor dynamic problems often involve changes in design speed and number of turbine or compressor stages. These approaches, however, as well as those involving the shaft and bearings, result in increased engine size and weight, not to mention increased costs due to the additional aerodynamic hardware, bearing supports, seals, and lubrication and cooling systems requirements.

Received July 31, 1974; revision received February 12, 1975. The contract efforts upon which this paper is based were conducted by Mechanical Technology, Inc., and Pratt & Whitney Aircraft Division of United Aircraft Corporation under USAF Contract F33615-72-C-1801. The work was administered under the direction of the Air Force Aero Propulsion Laboratory with E. A. Lake (AFAPL/SFL) acting as Project Engineer. The following members of the MTI Technical Staff were responsible for the multiplane-multispeed balancing efforts: J. M. Tessarzik, Senior Development Engineer; W. G. Spodnewski, Dynamics Test Specialist; and F. Gilham, Engineering Analyst.

Index categories: Aircraft Powerplant Design and Installation; VTOL Powerplant Design and Installation; Airbreathing Engine Testing.

*Mechanical Engineer-Analyst.
†Manager, Machinery Dynamics Center.
‡Assistant Project Manager, Pratt & Whitney Aircraft Division.

As the speed of the inner shaft increases to achieve increasingly higher engine performance, dynamic control becomes more difficult, if not impossible, to achieve by these convential means. In contrarotating two-spool engines, the increased speeds are resulting in intershaft bearing DN values which approach the current state-of-the-art. In the smaller two-shaft engines, regardless of whether contrarotation or corotation is used, the limited intershaft space is making it more and more difficult to incorporate the necessary bearing lubrication and seal systems. Furthermore, the continuing increase in operating temperatures further aggravates difficult bearing lubrication and cooling problems. The debris resulting from lubricant oxidation can cause catastrophic abrasive damage to bearings, seals, and shafts.

Inner Rotor Designs in Representative Advanced Engines

During the investigation of air bearings for advanced (1976), two-spool gas-turbine engines for the U.S. Army,[1] engine sizes from 2 to 5 lb/sec were considered. It was identified that the inner rotor shaft in a typical engine of this size would, at the design speed of 24,000 rpm, run between the second and third bending critical speeds. Recent design studies by Pratt and Whitney Aircraft (P&WA) of a similar size engine indicate an even worse problem because the inner rotor is designed to operate at higher speeds. For these engines, no way is seen to increase the inner rotor size or to incorporate interspool rolling-element bearings without some performance and mechanical penalty.

Intershaft vibration problems have also been identified for the advanced (1975–1980) V/STOL and complex-cycle engines. In fact, on the high-performance air bearing study for complex-cycle engines,[2] it is possible that the rotor dynamics of the two-spool engine (STFRJ-368) could have been improved if some form of intershaft vibration control bearing had been incorporated.

Control of Inner-Spool Dynamics

Since it is apparent that speeds and temperatures will continue to increase, other means of controlling the inner

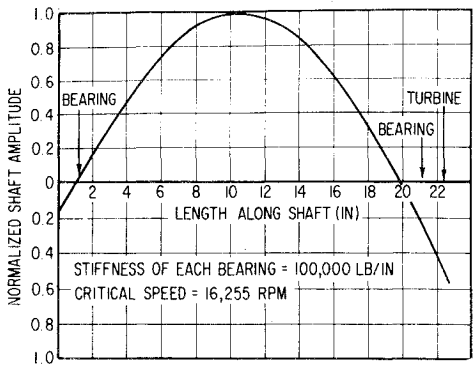

Fig. 1 Undamped shaft deflection mode at the first critical speed of the 17.5-to-1 engine power turbine rotor-bearing system.

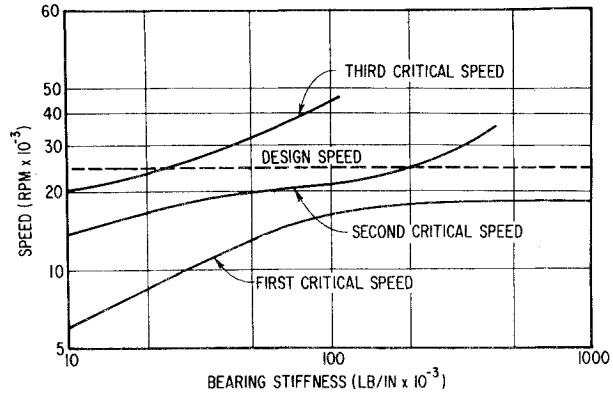

Fig. 2 Critical speed map for the power turbine rotor-bearing system studied by MTI and P&WA under U.S. Army Contract DAAJ02-69-C-0062.

spool vibrations need to be developed. It is currently envisioned that acceptable DN values can be increased from the current limit of about two million to the order of three million in the next few years by advances in material and fabrication technology. It is also possible that fluid-film bearings, which have no inherent speed limit (except for stability considerations), could be utilized as vibration control bearings. Both bearing types, however, must rely on a fluid for lubrication and cooling. Thus, the temperature capability of the organic lubricant appears to be the ultimate limiting factor. Currently, oil temperatures must be limited to about 350–400°F to prevent excessive oxidation. Advanced synthetic organic lubricants have achieved limited success in the 500–600°F range for periods of a few hours. The outlook for extending this temperature in an oxidizing environment to higher, more useful ranges, is not encouraging. Other current exploratory efforts are considering the use of ceramic components, which can operate without lubrication at greatly-elevated temperatures. Finally, there is the growing realization that engine operating speeds need not be restricted to values lower than the bending critical speeds if the engine is properly designed (e.g., if dampers are provided and the rotor is adequately balanced). Indeed, several new engines have been designed for precisely this mode of operation.

However, once the decision is taken to operate in the subcritical dynamic regime (the traditional approach), the utilization of air-lubricated intershaft bearings in place of the oil-lubricated rolling-element type becomes an attractive approach to controlling the vibration of the inner rotor. Immediately, the limitations due to oil temperature requirements and seals are eliminated. Temperature is limited only to the capabilities of the bearing surface and structural materials—currently 1000–1200°F. Furthermore, air bearings are not inherently speed limited and can be utilized in either corotating or contrarotating concentric-shaft arrangements.

The dynamic simulator hardware described in this paper has been used to date for the experimental evaluation of a stationary air-lubricated vibration control bearing concept.[3] A detailed report of the results of these tests will be the subject of a future paper, as will the results of other test programs. The techniques employed to design and make operational the simulator, together with a brief review of its first successful application, constitute the body of this paper.

Selection of Advanced Gas-Turbine Engine Configuration for Simulation

A preliminary investigation of two advanced gas-turbine engine configurations was made prior to selection of a representative design for simulation. The two engines were dynamically similar, in that each displayed dynamic characteristics which are symptomatic of a single problem: the power-turbine rotor design speed tends to lie above one or more shaft bending critical speeds. The representative advanced gas-turbine design finally selected for simulation also displayed this same characteristic problem.

The two engines examined were as follows. 1) a 10:1 turboshaft derivative for which P&WA prepared an assessment of the level of difficulty associated with attempting to avoid the critical speed problem through redesign; and 2) a 17.5:1 turboshaft advanced engine resulting from a joint MTI/P&WA air-bearing investigation.[1] The second of these two investigations will now be described.

17.5:1 Turboshaft Advanced Engine

Critical speed calculations for the 17.5:1 engine design were made to illustrate the dynamic characteristics of this class of engine. The rotor vibration mode shape at the first critical speed is shown in Fig. 1, in which it may be seen that the rotor is experiencing strong bending at this critical speed. A complete critical speed map for this shaft-bearing system is shown in Fig. 2, in which it may be seen that design speed lies above two bending critical speeds for bearing stiffnesses between 20,000 and 200,000 lb/in.

Advanced Gas-Turbine Configuration Considered During Preliminary Investigation

Based upon the foregoing engine characteristics, an advanced gas-turbine engine, shown in Fig. 3, was subjected to a dynamic analysis. The gas-generator section of this engine consists of one centrifugal compressor stage and a single-stage axial turbine and is optimized at 60,000 to 70,000 rpm. The power turbine rotor which is driven by two axial-flow turbine stages, is designed to operate at about 35,000 rpm. This rotor consists of a long, slender shaft, supported on two rolling-element bearings, and

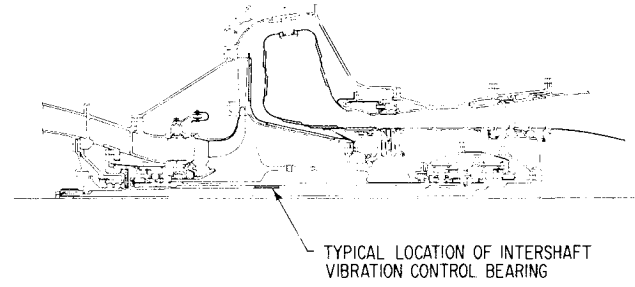

Fig. 3 Advanced engine selected for investigation of pneumomechanical critical speed control for gas turbine engine shafts.

carrying a single wheel outboard of the turbine-end bearing.

In the dynamic analyses made on the power turbine rotor, it was determined that the dynamic performance of the rotor could be improved by adding an intershaft vibration control bearing. Whereas two-bearing operation was above two bending critical speeds, the control bearing increased the criticals such that the design speed was well below the rotor's second bending critical. It should be noted that the lack of compressor wheels on the power turbine shaft of the engine shown in Fig. 3 provides for almost complete freedom in the location of the vibration control bearing along the rotor axis. This particular feature makes this type of engine an ideal vehicle for studying the utility of an intershaft bearing.

Design of Simulator

The dynamic simulator, while intended for eventual use in a two-spool configuration, initially employs a single rotor rather than the complete two-spool arrangement. This configuration was selected because the single rotor has good accessibility for balancing and for the mounting of probes which can be used to sense both vibration amplitudes and phase angles. The vibration characteristics of a single rotor are considerably less complex than those of a two-spool configuration, particularly one in which a radial interconnection between spools may exist. Test parameters (e.g., test configuration, temperatures, etc.) may be selected more easily and controlled much more precisely in a single rotor test.

Simulator Elements

The dynamic simulator assembly consists of several major components: the test rig base plate, the rolling-element bearing support housings, the air-lubricated foil bearing housing, the turbine and inertial wheel housings and the test rig rotor assembly. The aluminum test rig base plate provides a common surface to attach and align the various components, as well as a convenient and easily transportable method of assembling and aligning the various components prior to installation of the test rig in the space-limited test facility. The rolling-element bearing supports provide the mounting points for the ball bearings, labyrinth seals and the proximity probes. These housing designs also provide for the proper distribution and scavenging of the lubricant to the bearings, and for additional flexibility and damping of the ball bearing pedestal housings. Each of the two support housings was fastened securely to the test rig base plate. Pedestal flexibility is provided by the circumferentially located brazed-in pins attached to the bearing support plate located at the opposite end of the housing.

The turbine housing provides for the proper distribution of high-pressure air to the eight turbine nozzles and supports the electromagnetic pickup used to monitor shaft speed. The wheel housing design provides for the proper evacuation of the housing chamber to reduce the ambient air pressure and thus reduce air friction losses. It also supports both the sensor used to generate the reference signal for phase angle measurements and the proximity probes used to measure vibration of the simulator wheel.

The simulator rotor assembly consists of a long, slender shaft upon which are fastened an air-driven turbine wheel and the inertial disk. These three components are shown assembled in the upper portion of Fig. 4. The rotor is supported by two matched pairs of angular contact ball bearings.

Dynamic Analysis of the Simulator Rotor-Bearing Design

The primary indicators of dynamic similarity between two different shaft-bearing systems are the critical speeds of the rotor-bearing systems and their corresponding mode shapes. The dynamic similarity of the simulator rotor, from the initial design through to final design, was constantly evaluated and compared with the representative power turbine rotor design described.

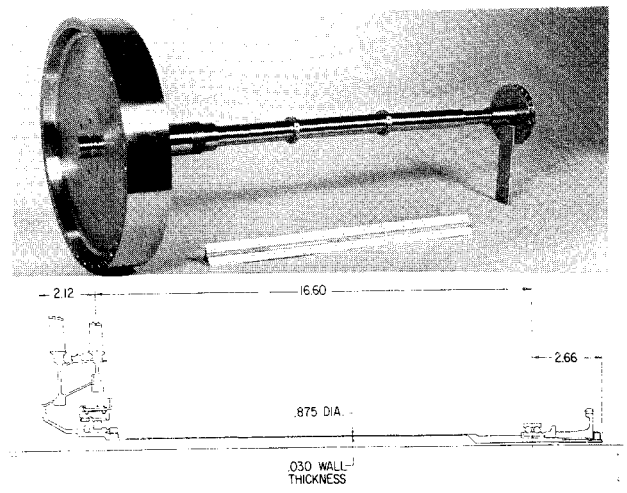

Fig. 4 Dynamic simulator rotor assembly (top) and advanced gas-turbine engine power turbine shaft cross-section.

Nominal Power Turbine Shaft Dynamic Properties.

The power turbine shaft design selected as being typical of the advanced gas-turbine engines previously described appears in the lower portion of Fig. 4. This rotor assembly consists of a very long hollow slender shaft to which is attached two axial turbine stages at one end. The power turbine is supported on rolling-element bearings at each end and is unsupported along the center portion of the rotor. The simulator rotor was designed to simulate as closely as possible the dynamic characteristics of this nominal power turbine design. At the expected operating bearing and bearing support stiffnesses of 10^5 to 2.5×10^5 lb/in., the power turbine design speed of 31,000 rpm will lie above the first two critical speeds. As shown in Fig. 5, these first two criticals involve significant shaft bending.

Simulator Rotor Design

The simulator rotor as illustrated in Fig. 4 consists of a long (21.8 in.) slender (0.875 in. diam) precision ground steel shaft to which is fastened a 3.0 in. diam air-driven turbine wheel and a solid 10.2 in. diam disk. Balancing planes were also machined onto the shaft in the form of two rings having twelve flat areas each for the attachment of set screws circumferentially on the shaft. (These rings are clearly shown in Fig. 4.) One additional balancing plane is located at the turbine wheel and two planes on the sides of the flanged outer diameter of the solid disk.

1) Inertial disk design: The primary design objective for the large disk on the simulator rotor was the simulation of the moment of inertia and the mass properties of the two axial stage turbine wheels on the nominal power turbine rotor. This simulation was, of course, to be achieved at a reasonable stress level for the material selected. The disk which best represented the mass and inertial properties of the two axial turbine stages was made from titanium and is shown in Fig. 4. This disk is 10.2 in. in diam and 1.80 in. thick at the flanged outer diameter surface, the two sides of which are used as balancing planes. The calculated maximum stress level of approximately 66,000 psi occurred at the axial center line of the disk at the maximum speed of 36,000 rpm.

2) Turbine wheel design: As initially conceived, the simulator design envisioned an air impulse turbine as an

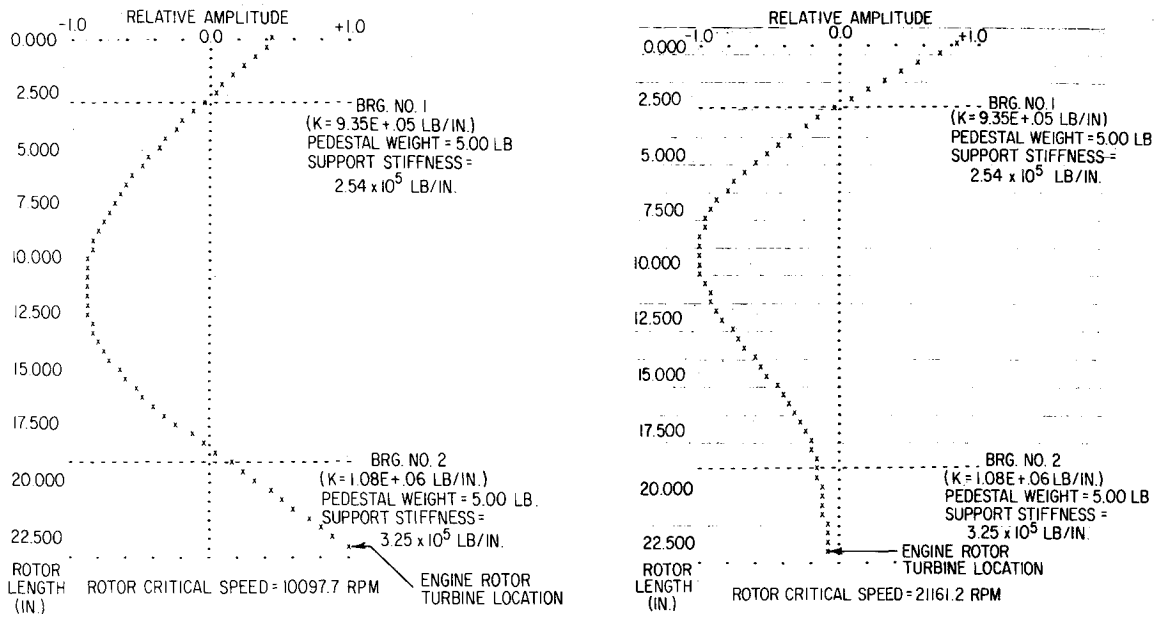

Fig. 5 Undamped mode shapes at first and second critical speeds at 10^5 lb/in. overall support stiffness for nominal power turbine rotor.

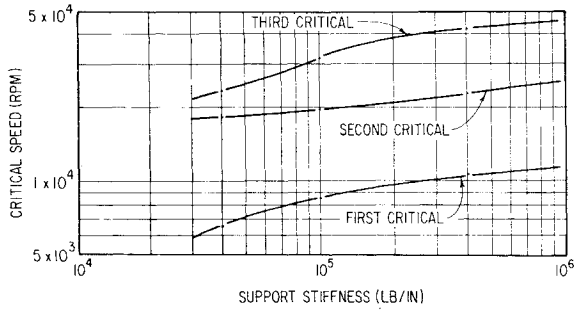

Fig. 6 Critical speed map for simulator rotor-bearing system.

integral part of the large titanium disk. The horsepower loss expected to be experienced by operating this wheel in ambient pressure air at full-speed, however, would have taxed severely the available plant air supply. Consequently, it was decided to partially evacuate the cavity around the titanium wheel and relocate the drive turbine to the opposite end of the rotor. Since the opposite end of the power turbine shaft already carried a small disk to simulate the weight and inertia of a gear, the relocation of the turbine did not cause a change in rotor characteristics. Calculations of air drag rotor horsepower losses indicated that 2.42 hp would be required to drive the rotor at 36,000 rpm, with the disk in a reduced atmosphere of 2 psia. The turbine was sized according to information supplied by Barbour Stockwell Company, Cambridge, Mass. For a nominal two-inch diameter turbine with atmospheric exhaust and a total nozzle cross-sectional area of 0.100 in.^{2}, a power output of 4 hp at 36,000 rpm and 90 psig air supply pressure was calculated.

3) *Critical speeds and mode shapes:* The critical speed map of the simulator rotor-bearing system is shown in Fig. 6. The titanium wheel was somewhat heavier than the nominal power turbine wheels. The effect of this upon the critical speed characteristics of the simulator rotor was to lower the simulator shaft-bearing system's critical speeds compared to those of the nominal rotor-bearing system.

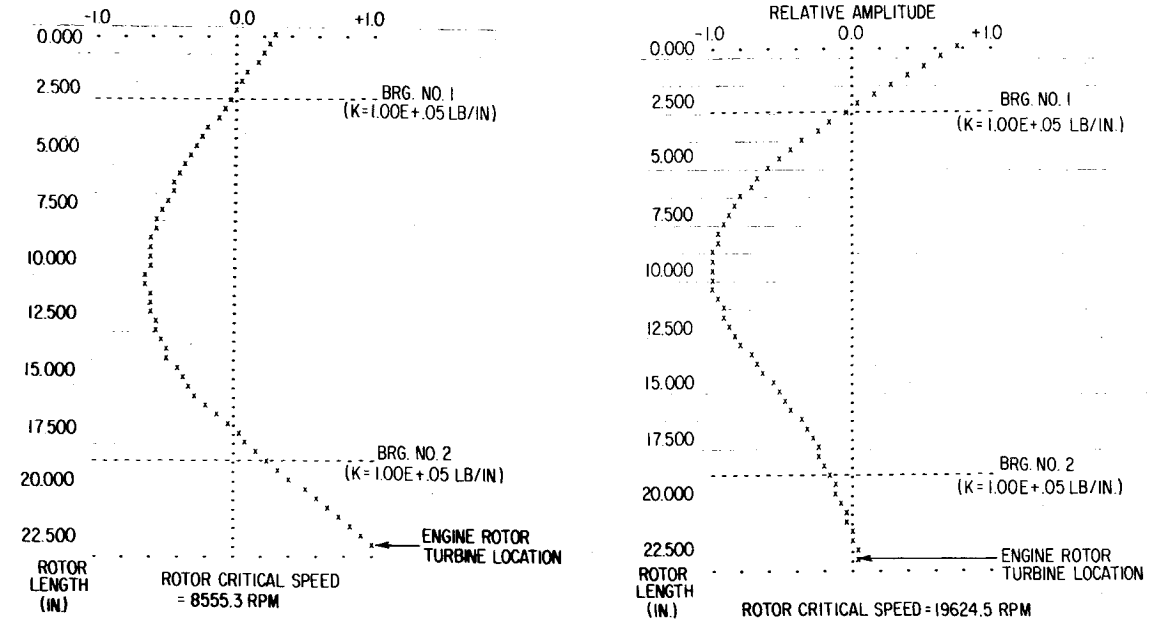

Fig. 7 Undamped mode shapes at first and second critical speeds at 10^5 lb/in. overall support stiffness for test rig rotor.

Table 1 Flexible mounts for simulator bearings

	17 mm Bearing	35 mm Bearing
Number of rods	12	12
Rod diameter, in.	0.283	0.301
Rod length, in.	1.75	1.75
Maximum rod stress, psi	19,060	20,200
Support spring stiffness, lb/in.	2.54×10^5	3.25×10^5
Combined Brg & Support Stiffness, lb/in.	200,000	250,000

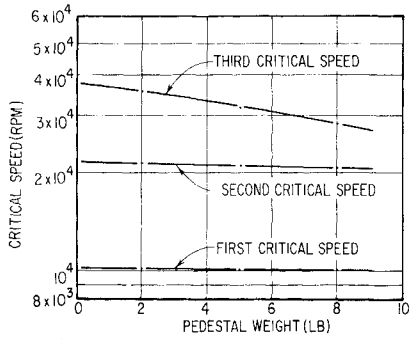

Fig. 8 Effect of pedestal weight on predicted critical speed for simulator rotor with nominal bearing and flexure pin pedestal stiffness.

The corresponding undamped normalized mode shape plots for the first two critical speeds at overall support stiffnesses (bearing and structure) of 10^5 lb/in. are shown in Fig. 7.

It may be noted through comparison of the predicted nominal power turbine shaft and simulator shaft mode shapes at 10^5 lb/in. overall stiffness, that the mode shapes for the first and second critical speeds are very similar for both systems. Achievement of this good matching of mode shapes for the two criticals of interest is also accompanied by the added benefit that the simulator's first critical speed occurs at a lower speed. This results in safer operation. Furthermore, the simulator's first and second critical speeds are well separated, which greatly facilitates balancing and interpretation of the test results.

Rotor Support System Design

Ball Bearings

The rotor support system design objective was to provide the simulator with a bearing system capable of sustaining rotation speeds to approximately 32,000 rpm and possessing a support stiffness that closely simulates the selected power turbine shaft design stiffness. In order to avoid possible problems with a roller bearing, two duplex angular contact ball bearing sets were selected for rotor support. Both ball bearing sets have inner diameters identical to the bearings on the power turbine shaft design shown in the lower portion of Fig. 4.

The large diameter (35 mm) bearing pair next to the titanium rotor disk is clamped to the bearing housing, while the opposite bearing pair (17 mm) is free to float axially in its housing. Both sets are installed in a back-to-back configuration. Oil jet lubrication and cooling is provided through orificed jet holes provided in each of the spacer rings mounted between the two individual bearings of each set. A summary of bearing characteristics, including calculated data for bearing life and bearing stiffness, may be found in Ref. 3.

Ball Bearing Support Springs

The estimated combined bearing-support stiffness values for the nominal engine design were 200,000 lb/in. for the 17 mm bearing and 250,000 lb/in. for the 35 mm bearing. Since the calculated simulator bearing stiffness values for the bearings alone were 9.35×10^5 and 1.085×10^6 lb/in., respectively, individual spring supports were designed to lower the combined bearing-support stiffness values to the range of the nominal engine design values. This was accomplished by circumferentially brazing-in the end of a number of small diameter rods into the rolling-element support housing and also brazing-in the opposite end into the bearing support plate which supports the ball bearings in their own housing. The stiffness of this squirrel-cage-type bearing spring support was then calculated as a set of parallel, fixed end, cantilevered beams whose free end was not permitted to rotate. The results are shown in Table 1.

Using the calculated support spring stiffnesses indicated in Table I in series with the bearing stiffnesses, additional critical speed calculations and mode shapes were obtained to determine the effect of pedestal mass on the first three critical speeds. Pedestal masses of 2, 5, and 8 lb were considered in these calculations. The effect of variable pedestal

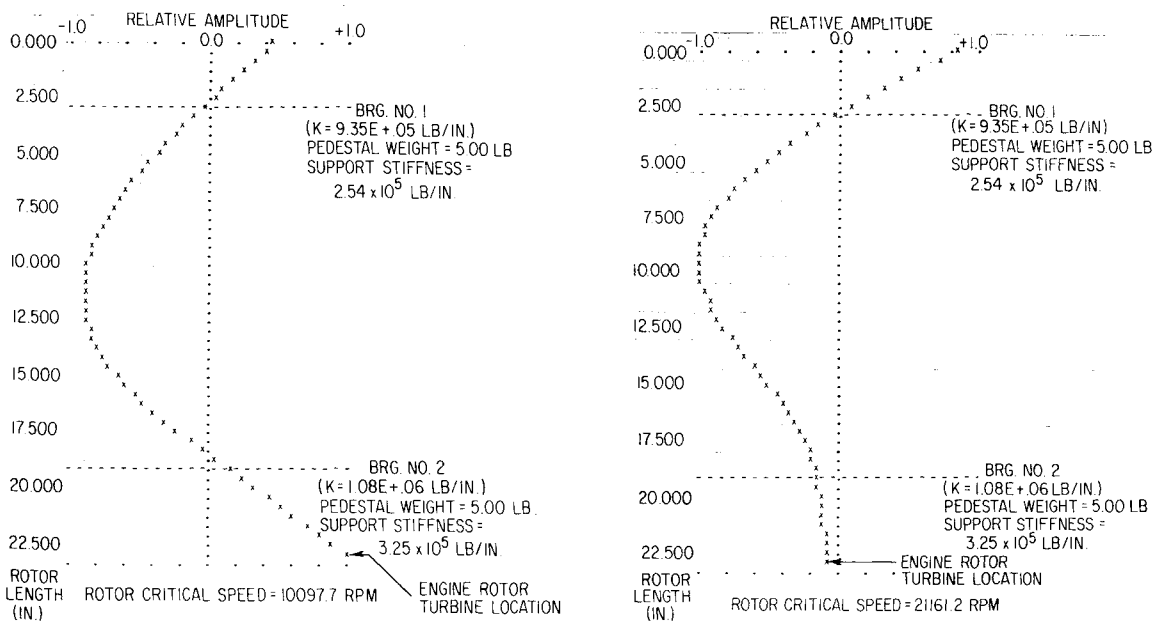

Fig. 9 Undamped mode shapes at first and second critical speeds of test rig rotor considering pedestal mass and flexure pin supporting stiffnesses as indicated.

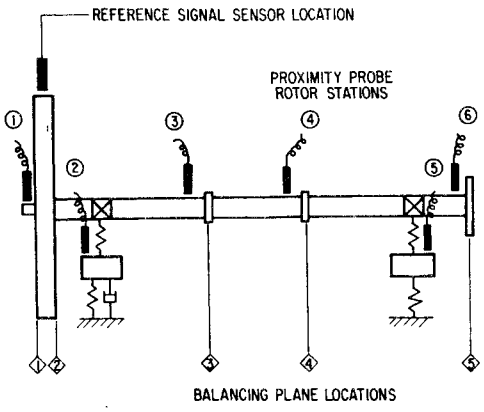

Fig. 10 Probe and balancing plane locations.

mass on the first three critical speeds is summarized in Fig. 8 at the nominal bearing and support stiffnesses previously indicated.

The undamped rotor mode shapes for the test rig rotor-bearing system with pedestal masses of five pounds and supporting spring stiffnesses as previously indicated are shown in Fig. 9. These mode shape plots were also found to be typical for the cases considering pedestal masses of 2 and 8 lb with the same supporting spring stiffness values.

Preparation and Operation of the Dynamic Simulator

The primary objective of the first series of tests to be performed with the simulator was to obtain an evaluation of the dynamic behavior of air-lubricated foil bearings for future use as intershaft vibration control bearings. The function of these bearings, as described in earlier sections, was to provide enough radial stiffness to shift the rotor-bearing system's second bending critical speed above the design speed. The primary means of obtaining this data was to be by comparison of before and after vibration behavior of the rotor, without and with the test bearing, respectively.

In order that such a comparison be meaningful, the rotor-bearing system's dynamic behavior must be shown to be repeatable before and after the bearing test. An effective manner for achieving this repeatability is to provide for insertion and removal of the test bearing without disassembly and reassembly of the rotor-bearing system. Such disassembly-assembly, in spite of care used and hardware precision level employed, often causes changes in either the system's balance or damping. The results of any before-after tests which involve disassembly and reassembly, may therefore be compromised. Following manufacture of the shaft, disk, and other components, the rotor-bearing system was assembled without balancing. This step could be omitted because of the availability of Multiplane-Multispeed Balancing capability, which permits balancing after assembly at any desired speed(s).

Prior to conducting the first series of tests on the simulator, preliminary runs were made to permit the test personnel to become familiar with the operating characteristics of the rotor and the auxiliary supporting control systems. The turbine drive system, the self-contained lubrication-cooling system, the vibration-amplitude inductive probe system, the speed and phase reference signals, and the electronic data acquisition system were checked out during these preliminary runs. Once the controlability of the test rig and its supporting systems had been proven, balancing operations were conducted on the test rig rotor.

Simulator Rotor Balancing

Balancing of the simulator rotor was performed through the use of multiplane-multispeed balancing technology,

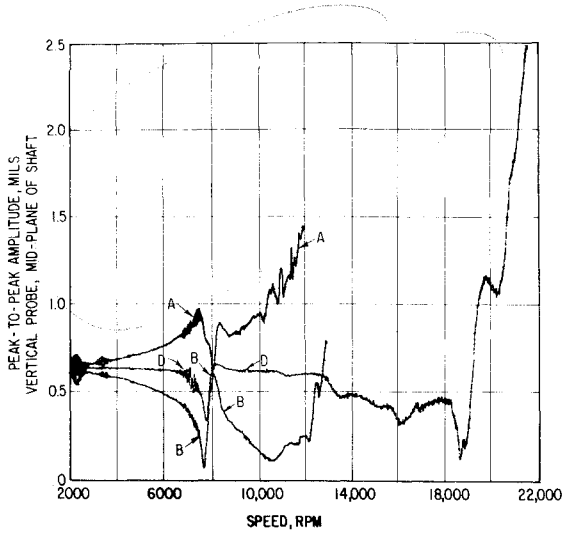

Fig. 11 Vertical rotor amplitudes at station 3: initial condition (as manufactured) and after the first and third balancing runs using planes 1, 2, and 5.

which had recently become available as a result of contract efforts supported by the NASA Lewis Research Center. This advanced balancing method has been developed for cost-effective multiplane balancing of gas-turbine rotors[4-11] which must operate in the vicinity of one or more bending critical speeds.

The simulator rotor design permits simultaneous balance corrections to be made in each of five correction planes. The first balance correction run, which was made using balancing planes 1, 2, and 4 (Fig. 10) was designed to suppress rotor vibrations at a speed of 10,400 rpm. Vibration sensors 1, 4, and 6 were used to obtain data for this correction. Two additional balance correction runs were also made using the same planes at higher speeds. The results of these initial balancing runs are shown at the midshaft vertical plane in Fig. 11. In this and subsequent figures, curve A denotes amplitudes for the unbalanced rotor, curve B for rotor amplitudes after one balancing run, curve C for rotor amplitudes after two balancing runs, and curve D for rotor amplitudes after three balancing runs.

During these balancing runs, it was confirmed that it would be necessary to evacuate the turbine simulator wheel housing to operate the simulator to the design speed of 32,000 rpm. In the initial balancing runs, a maximum speed of 14,900 rpm was attained at a turbine air supply of 85 psig with the disk housing at atmospheric pressure. This data confirmed the design performance of the turbine drive system. Connection of the vacuum pumping system to the housing chamber permitted operating speeds up to 23,000 rpm to be reached after the third correction weight run. Full design speed was subsequently achieved in a fully satisfactory manner.

System Response Tests

A series of tests were next conducted, including several of preliminary foil bearing configurations, to better understand the dynamics of the test rotor bearing system, with particular emphasis on the influence of the single squeeze-film damper (at the disk end bearing). Air, oil, and silicone fluids were placed in the damper to determine the influence of the damper on the test rig system. It was found that the amount of damping achieved was time dependent, and that the damping was affected by the operation history in terms of vibration energy dissipation. It was found that the desired degree of test data repeatability could not be obtained when the damper was used, primarily because of damper heating effects. It was concluded from these tests that all future tests should be con-

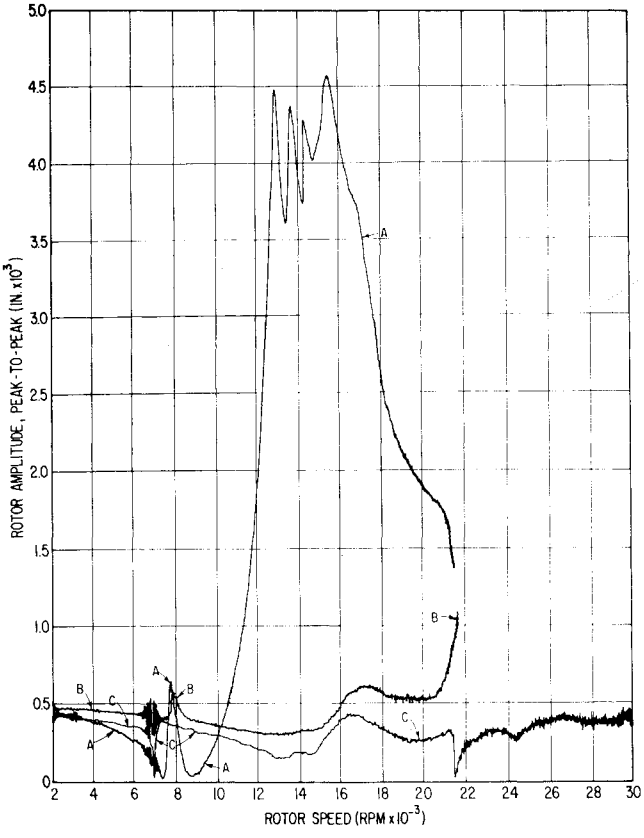

Fig. 12 Vertical rotor amplitudes at sensor 1: initial condition (as manufactured) and after two consecutive balancing runs.

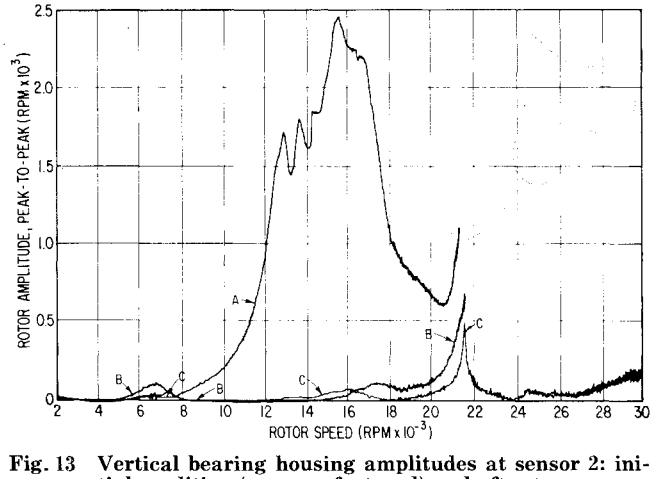

Fig. 13 Vertical bearing housing amplitudes at sensor 2: initial condition (as manufactured) and after two consecutive balancing runs.

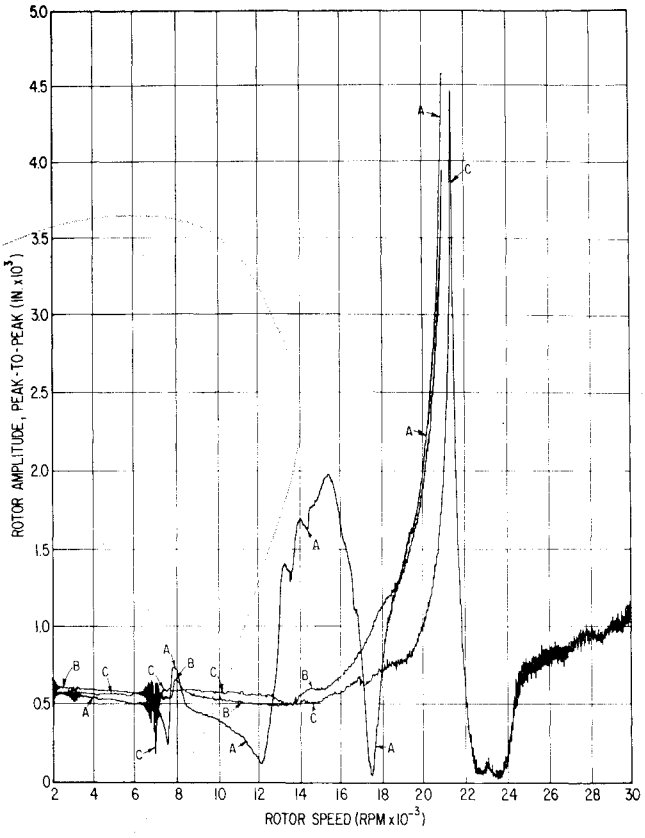

Fig. 14 Vertical bearing housing amplitudes at sensor 4: initial condition (as manufactured) and after two consecutive balancing runs.

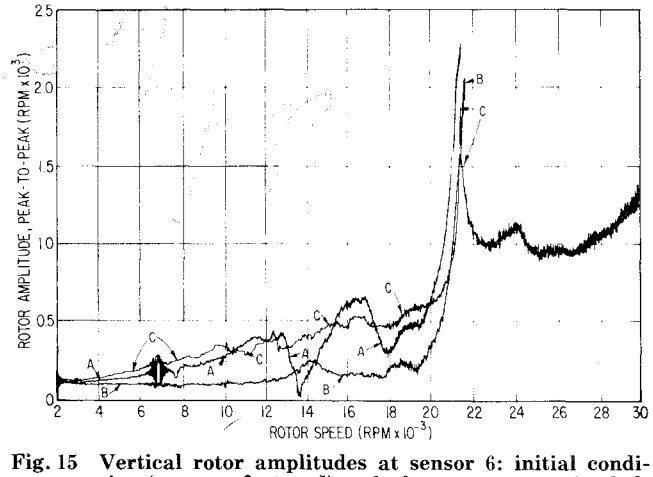

Fig. 15 Vertical rotor amplitudes at sensor 6: initial condition (as manufactured) and after two consecutive balancing runs.

ducted without the damper. This could be done by providing a continuous supply of low-pressure air instead of oil to the damper. In this way, the results of the remaining bearing dynamic tests would be unaffected by possible temperature and pressure variations in the damper. While operation of an undamped rotor bearing system through two undamped bending critical speeds may appear to be a difficult and dangerous undertaking, this is no longer the case. Multiplane-multispeed balancing permits this to be done on a routine basis.

At the same time the tests were conducted to determine the effect of energy dissipation in the damper, it was noted that further balance deterioration had occurred. It was thus decided to rebalance the test rotor. An initial rebalancing effort was conducted with four balancing planes, and with three lateral vibration sensors, much the same way as the initial balancing had been accomplished. However, it quickly became obvious that the Balancing System was "chasing" a small, moveable unbalance in the drive turbine. A check of the turbine mounting quickly confirmed that the turbine locking nut had in fact not been fully tightened during initial assembly. This was quickly remedied. It is specifically noted that this usage of the Balancing System illustrates the capability of diagnosing rapidly and precisely the location and amount of unbalance in an operating system. Prior to rebalancing, correction weights from all of the prior balancing runs were removed. In addition, a fourth lateral vibration sensor was added near the center of the rotor (see Fig. 10) at probe station 3. Balancing was then conducted in two steps, the results of which are illustrated in Figs. 12–15. Note that each correction was a five-plane correc-

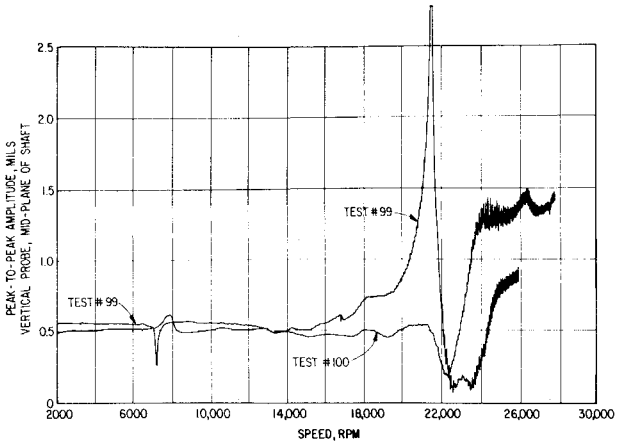

Fig. 16 Vertical rotor amplitudes at sensor 4: initial base line condition and with air-cooled three-pad hydrodynamic resiliently-supported foil bearing.

tion, with inputs from four sensor planes. The first correction using data taken at about 14,000 rpm suppressed the large peak amplitude in the 15,000 rpm range (tentatively identified as a pedestal resonance). The second correction using data taken at about 15,000 and 21,000 rpm was used to keep the earlier 15,000 rpm peak fully suppressed and to enable the rotor to operate through the second critical speed at about 21,000 rpm. As shown by the 'C' responses in Fig. 14, this procedure very nicely isolated the second critical speed peak so that the effectiveness of the air-lubricated intershaft foil bearing in raising this critical speed could subsequently be assessed. It may be noted that the amplitude peak in the 24,000 to 28,000 rpm range was also tentatively identified as a pedestal resonance.

Brief Summary of Air-Lubricated Foil Bearing Tests

Using the simulator as prepared above, a foil bearing was installed at the center of the rotor and several test runs made. Throughout these tests, foil temperatures were observed and evaluated. Air cooling enabled bearing operating temperatures to be maintained near room temperature level. The results of an important series of tests are shown in Fig. 16. These results are extremely satisfactory, in that they show the second critical speed to be moved entirely out of the rotor's operating speed range. Moreover, the results are repeatable. After the test, the bearing was removed, inspected, and cleaned, and returned immediately to the test rig. The rotor speed was then run up to 30,000 rpm and back down. The results were virtually identical to the earlier results, with both increasing and decreasing speeds.

Conclusions

The rotor-bearing system simulator described herein has been constructed to be representative of the inner spool of a large class of gas turbine engines: the front-drive power-turbine type typically utilized to drive VSTOL aircraft and helicopters. While the simulator is dynamically similar to a specific small advanced engine designed for possible future helicopter application, its properties may be utilized for scale studies of other engine sizes. In addition, with addition of simulated fan and compressor stages, and rearrangement of components, it may be utilized for simulation of turbofan and turbojet engines as well.

The simulator rotor carries a large overhung titanium disk and is mounted on two flexibly-mounted duplex bearing pairs, which are internally preloaded. One bearing is equipped with a squeeze-film damper. The rotor is driven by a small air turbine, with the large disk mounted within a chamber which may be evacuated. The simulator was designed on a modular basis in order to facilitate addition, removal, or changes of individual components without disturbing the entire assembly, and for balancing and rebalancing on the test stand without disassembly, through use of the Multiplane-Multispeed Balancing System.

The simulator has been successfully operated to design speeds of 32,000 rpm for extended periods of time at low vibration levels, both with and without the bearing squeeze film damper. This speed range encompasses two critical speeds at which considerable bending of the rotor elastic axis can occur, with associated lateral vibration levels which could have been quite severe in the absence of proper vibration energy control measures. This very successful behavior was obtained without traditional low-speed balancing of components, and with only one build-up of the system. The simulator has been utilized to date for proof-testing of a class of air-lubricated foil bearings for future use as intershaft bearings, designed to elevate the system's second bending critical speed above the rotor design speed range. That objective was achieved.

References

[1]Waldron, W. D., Young, W. E., and Curwen, P., "An Investigation of Air Bearings for Gas-Turbine Engines," USAAMRDL Tech. Rept. 71-59, Nov. 1971, U.S. Army Air Mobility Research and Development Lab., Fort Eustis, Va.

[2]Waldron, W. D. and Young, W. E., "High Performance Bearing Study," prepared under Air Force Contract F33615-71-C-1382 and issued as AFAPL-TR-72-63, July 1972, Air Force Aero Propulsion Lab., Wright-Patterson Air Force Base, Ohio.

[3]Cundiff, R. A., Badgley, R. H., and Reddecliff, J., "Pneumomechanical Critical Speed Control for Gas Turbine Engine Shafts," Tech. Rept. MTI-73TR42, prepared under Air Force Contract F33615-72-C-1801 and issued as AFAPL-TR-73-101, Nov. 1973, Air Force Aero Propulsion Lab., Wright-Patterson Air Force Base, Ohio.

[4]Tessarzik, J. M., "Flexible Rotor Balancing by the Exact Point-Speed Influence Coefficient Method," Tech. Rep. MTI-70TR59 prepared for NASA-Lewis Research Center under Contract NAS3-13473, Rep. CR-72774, Oct. 1970, NASA.

[5]Tessarzik, J. M., Badgley, R. H., and Anderson, W. J., "Flexible Rotor Balancing by the Exact Point-Speed Influence Coefficient Method," *ASME Transactions, Journal of Engineering for Industry*, Ser. B, Vol. 94, Feb. 1972, pp. 148–158.

[6]Tessarzik, J. M., "Flexible Rotor Balancing by the Influence Coefficient Method: Part 1—Evaluation of the Exact-Point-Speed and Least Squares Procedures," Tech. Rept. MTI-72TR32, prepared for NASA-Lewis Research Center Under Contract NAS3-14420, Rept. CR-121107, July 1972, NASA.

[7]Tessarzik, J. M. and Badgley, R. H., "Experimental Evaluation of the Exact Point-Speed and Least-Squares Procedures for Flexible Rotor Balancing by the Influence Coefficient Method," *ASME Transactions, Journal of Engineering for Industry*, presented at Design Engineering Technical Conference, Cincinnati, Ohio, Sept. 1973.

[8]Rieger, N. F. and Badgley, R. H., "Flexible Rotor Balancing of a High-Speed Gas Turbine Engine," SAE Paper 720741, Milwaukee, Wis., Sept. 1972.

[9]Badgley, R. H. and Rieger, N. F., "The Effects of Multiplane Balancing on Flexible Rotor Whirl Amplitudes," SAE Paper 730102, Detroit, Mich., Jan. 1973.

[10]Badgley, R. H., "The Potential Impact of Multiplane-Multispeed Balancing on Gas Turbine Production and Overhaul Costs," ASME Paper 74-GT-94, presented at the ASME Gas Turbine Conference, Zurich, Switzerland, March–April 1974.

[11]Badgley, R. H., "Implications of Multiplane-Multispeed Balancing for Future Turbine Engine Design and Cost," SAE Paper 740865, presented at the National Aerospace Engineering & Manufacturing Meeting of the Society of Automotive Engineers, San Diego, Calif., Oct. 1974.